

Final Scientific Report

For Project Titled:

Phase Transitions in  $(\text{Mg},\text{Fe})_2\text{SiO}_4$  Olivine under Shock Compression

Prepared For

United State Department of Energy

Office of Fusion Energy Sciences

Award: DE-SC0018925

Performance Period: September 1, 2018 – August 31, 2020

Prepared by:

Professor Thomas S. Duffy

Department of Geosciences and

Princeton Institute for the Science and Technology of Materials

Princeton University

Submitted: December 4, 2020

## **Disclaimer**

Any findings, opinions, and conclusions expressed in this report are those of the author and do not necessarily reflect the views of the Department of Energy.

## **Acknowledgements**

We thank the staff of the Materials in Extreme Conditions end-station at the Linac Coherent Light Source for experimental assistance. Use of the Linac Coherent Light Source, SLAC National Accelerator Laboratory, is supported by the U.S. Department of Energy, Office of Science, and Office of Basic Energy Sciences under Contract No. DE-AC02-76SF00515. This report is based upon work supported by the U. S. Department of Energy under award No DE- SC0018925.

## **Proprietary Data Notice**

This report does not contain any proprietary data.

## Executive Summary

The response of forsterite,  $\text{Mg}_2\text{SiO}_4$ , under dynamic compression is of fundamental importance for understanding its phase transformations and high-pressure behavior. Here, we have carried out an *in situ* X-ray diffraction study of laser-shocked polycrystalline and single-crystal forsterite from 19 to 122 GPa using the Matter in Extreme Conditions end-station of the Linac Coherent Light Source.

Under laser-based shock loading, forsterite does not transform to the high-pressure equilibrium assemblage of  $\text{MgSiO}_3$  bridgmanite and  $\text{MgO}$  periclase, as has been suggested previously. Instead, we observe forsterite and forsterite III, a metastable polymorph of  $\text{Mg}_2\text{SiO}_4$ , coexisting in a mixed-phase region from 33 to 75 GPa for both polycrystalline and single-crystal samples. Densities inferred from X-ray diffraction are consistent with earlier gas-gun shock data. At higher stress, the response is sample-dependent. Polycrystalline samples undergo amorphization above 79 GPa. For [010]- and [001]-oriented crystals, a mixture of crystalline and amorphous material is observed to 108 GPa, whereas the [100]-oriented forsterite adopts an unknown phase at 122 GPa. The first two sharp diffraction peaks of amorphous  $\text{Mg}_2\text{SiO}_4$  show a similar trend with compression as those observed for  $\text{MgSiO}_3$  in both recent static- and laser-driven shock experiments.

This study provides new insight into the transformation of forsterite under nanosecond-duration shock loading. This work emphasizes the importance of formation of metastable phases along the Hugoniot and adds to evidence that the 300-K single-crystal diamond anvil cell experiments have relevance for understanding structures formed under shock compression. In particular, the metastable phase forsterite III has now been shown to form under dynamic compression from 10s to 100s of nanoseconds as well as under 300-K static compression. Upon compression to higher pressures,  $\text{Mg}_2\text{SiO}_4$  transforms to an amorphous phase. These results have broad relevance for understanding the behavior of silicates under dynamic compression.

## Introduction

Mg-rich olivine,  $(\text{Mg},\text{Fe})_2\text{SiO}_4$ , occurs widely in igneous and metamorphic rocks, and is the dominant phase in Earth's upper mantle [1]. The physical properties of liquid  $\text{Mg}_2\text{SiO}_4$  are important for modeling partial melting of the mantle and the behavior of magma oceans. In addition, olivine is a common constituent of terrestrial planets and meteorites.

Static-compression experiments have shown that at high pressure and temperature ( $>1000$  K),  $(\text{Mg},\text{Fe})_2\text{SiO}_4$  adopts a spinelloid structure (wadsleyite) at about  $\sim 14$  GPa, and then transforms to a spinel structure (ringwoodite) at  $\sim 18$  GPa. At 24 GPa, ringwoodite dissociates into  $(\text{Mg},\text{Fe})\text{SiO}_3$ , bridgmanite and  $(\text{Mg},\text{Fe})\text{O}$ , ferropericlase which are expected to be the major phases of Earth's lower mantle. These phase transitions in the  $(\text{Mg},\text{Fe})_2\text{SiO}_4$  system are the primary cause of the major seismic discontinuities at 410-, 520-, and 660-km depths in the Earth's mantle [1]. These discontinuities play a key role in controlling the dynamics and heat flow in the Earth's interior [1].

Metastable polymorphs of forsterite,  $Mg_2SiO_4$ , the Mg end-member of olivine, have also been reported at high pressure. A 300-K single-crystal X-ray diffraction (XRD) study showed that forsterite (orthorhombic,  $Pbnm$ ) transforms to forsterite II (triclinic,  $P1$ ) and forsterite III (orthorhombic,  $Cmc2_1$ ) at 50 and 58 GPa, respectively [2]. Fo III is related to the post-spinel calcium titanate structure and has fully 6-coordinated silicon. It remains metastable to above 100 GPa at ambient conditions.

Due to the geophysical importance of Mg-rich olivine, there has been much interest in understanding its shock-compression behavior. The Hugoniot of forsterite has been interpreted to reflect transformation to a high-pressure phase through a broad mixed-phase region that begins at about 50 GPa and is completed near 100 GPa [3]. This stress is much greater than that required for transformation of olivine in static experiments, suggesting a role for kinetics on the short timescales of shock experiments. The metastable Fo III phase has been reported in recent gas-gun experiments at 44 and 73 GPa based on *in situ* XRD data [4]. However, the exact natures of the mixed-phase and high-pressure phase regions are still not well understood.

Constraining the behavior of olivine under dynamic loading is necessary for understanding its metastable states, transformation pathways and kinetics, structural polymorphism, and equations of state, which all play a role in interpreting geophysical phenomena. Here, we report the results of *in situ* XRD measurements on laser-shock experiments on forsterite samples covering a wide stress range.

## Experimental Approach

### Sample Preparation

Synthetic single-crystal and polycrystalline Fo ( $Mg_2SiO_4$ ) samples cut into  $1\text{ mm} \times 1\text{ mm} \times \sim 50\text{ }\mu\text{m}$  slices were used in this study. The single-crystal samples (Roditi International, unit-cell volume  $V_0=290.0\text{ \AA}^3$ ) were cut from a  $10 \times 10 \times 10\text{ mm}^3$  cube, with the main face of each slice oriented normal to the  $a$ -,  $b$ -, or  $c$ -axis. The fully dense, synthetic, sintered polycrystalline aggregates from the same source as used in Newman et al. [4].

### Laser Shock Experimental Configuration

Laser-driven shock-compression experiments were performed at the Matter in Extreme Conditions (MEC) end-station of the Linac Coherent Light Source (LCLS) at the Stanford Linear Accelerator Center [5]. Target packages consisted of a polyimide (CH) ablator glued to a Fo sample with or without a LiF window epoxied to the rear surface (Figure 1). Samples were shock compressed using one or both of the lasers from a two-beam 527-nm Nd:glass laser system. The laser pulses were 10–15 ns in duration with a quasi-flat-top shape. Experiments were performed both with and without phase plates. The shock stress was varied from 19 to 122 GPa by tuning the laser spot size, pulse length, and laser energy. Pulse shapes were monitored to assess the reproducibility of the drive conditions for a given laser energy, pulse length, and spot size.

## Stress Determination

The forsterite free-surface or Fo/LiF-interface velocity was monitored by a line-imaging velocity interferometer system for any reflector (VISAR). The VISAR provided information on the shock arrival time, spatial planarity, and peak elastic stress. For a given drive condition, the peak stress in a sample backed by a LiF window was determined by impedance matching. As the strength of forsterite on the Hugoniot is poorly constrained, we have not made any correction for the difference between axial stress and mean pressure. Hydrodynamic simulations were performed using the one-dimensional hydrocode, HYADES, to provide additional constraints of the stress evolution on compression and release.

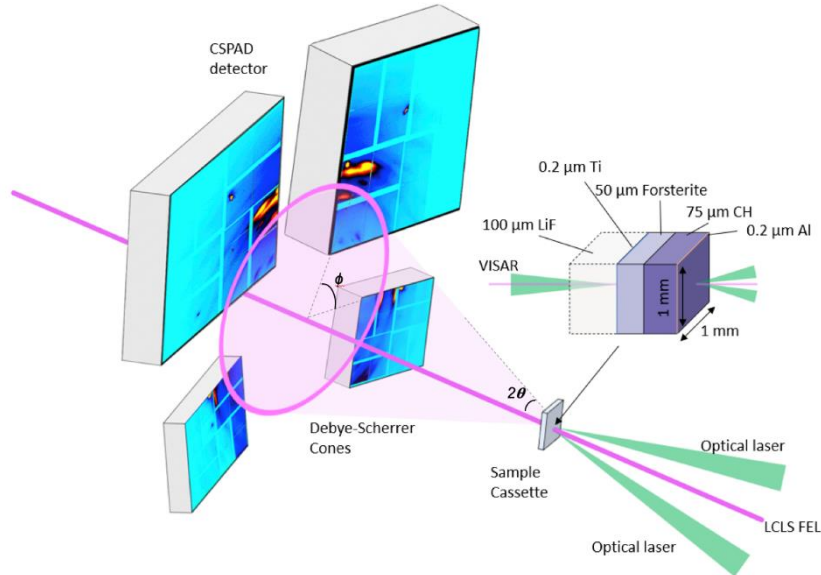


**Figure 1.** Schematic of the experimental setup for X-ray diffraction under laser-driven shock compression.

## X-ray Diffraction Analysis

Samples were probed by angle-dispersive X-ray diffraction. The LCLS provided quasi-monochromatic 8.5 keV X-ray pulses of 60-fs duration, each containing  $10^{12}$  photons. The X-rays were focused to a spot size of  $\sim 20$  μm at the center of the laser drive. Diffraction peaks from the sample were recorded on four Cornell-SLAC Pixel Array Detectors. The CSPAD images were integrated azimuthally to convert them to one-dimensional XRD patterns. CeO<sub>2</sub> and LaB<sub>6</sub> were used as standards to calibrate the sample-to-detector distance and the orientation of each detector.

A single XRD pattern was collected during each shock-compression experiment. A time series of diffraction patterns was collected by changing the XRD probe time on a sequence of shots using the same drive conditions and nominally identical targets with and without a LiF window. The stress for the series of shots was determined from the target with a LiF window. Diffraction peak

assignments were initially made by comparing the observed peaks to predicted peak positions based on 300-K static data at similar pressures. Lattice  $d$ -spacings were obtained by peak fitting, and unit-cell parameters were refined by least-squares fitting.

## Results

Compressed forsterite was identified in XRD patterns collected from single crystals shocked to 19 GPa and 25 GPa. At 33 GPa, new peaks were observed that could be assigned to the metastable phase Forsterite III. These results are in agreement with recent *in situ* XRD results from gas-gun experiments, which first reported evidence for the formation of Fo III during shock loading of forsterite [4].

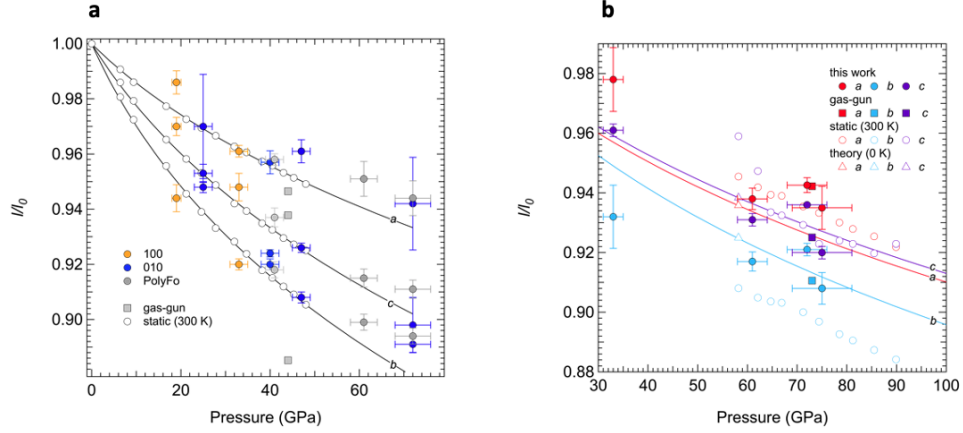


**Figure 2.** Relative unit-cell axial lengths of (a) forsterite and (b) forsterite III under shock and static compression.

Forsterite III peaks were observed for all four types of starting materials when shock-compressed to stresses in the range of 33 to 75 GPa. Figure 2 shows the relative lattice parameters determined for Fo and Fo III in this study compared with previous shock (gas-gun) and static-compression data. Although there are uncertainties in the shock-wave data due to the spotty nature of the patterns as well as stress uncertainty, the lattice parameters are generally consistent with static data and *ab initio* computations [6].

Figure 3 shows densities obtained from our XRD measurements compared with those measured at the continuum level from gas-gun experiments. Beginning at 28 GPa, continuum Hugoniot states become at first slightly and then increasingly denser than forsterite at 300 K, consistent with the appearance and growth of the denser polymorph, as observed in our XRD data. Above 60 GPa, the densities of Fo III determined from our X-ray data are similar to static-compression results for this phase [2].

Our results for  $\text{Mg}_2\text{SiO}_4$  are similar to those reported recently for [100]-oriented single crystal enstatite,  $(\text{Mg},\text{Fe})\text{SiO}_3$ , under nanosecond laser shock compression where a mixture of enstatite and a dense pyroxene-like phase was observed up to 80 GPa [7]. The dense phase is suggested to be similar to the  $\beta$ -post-opx phase identified in 300-K single-crystal diamond cell experiments [8]. Thus, both enstatite and forsterite appear to adopt a phase mixture over similar stress ranges on the Hugoniot composed of a compressed low-pressure phase and a high-pressure phase that corresponds to the metastable phase found in low-temperature diamond cell experiments. This indicates that mafic silicates may exhibit similar behavior under shock loading and highlights the role of metastable phases along the Hugoniot at nanosecond timescales.

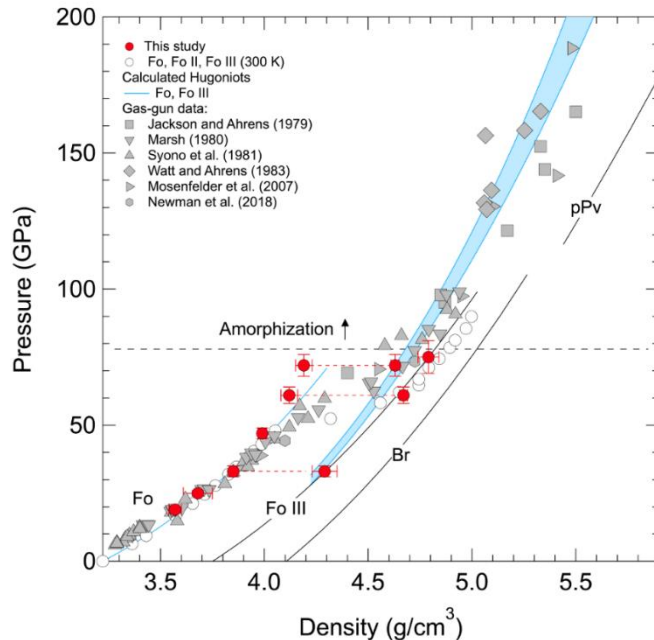


**Figure 3.** Densities determined from the present data (red symbols) compared to continuum gas-gun results.

Upon compression of polycrystalline forsterite above 79 GPa, we observe only broad untextured features that we interpret as amorphization of the sample. For [010] and [001] single crystals compressed to 108 GPa we observe evidence for significant disordering but not complete amorphization. In contrast, [100]-forsterite shocked to a peak stress of  $122 \pm 24$  GPa retains a high degree of crystallinity.

Diffraction data from silicate glasses are generally characterized by a broad peak at low values of the scattering vector,  $Q$ , known as the first sharp diffraction peak (FSDP). Under compression, a second feature (2<sup>nd</sup> sharp diffraction peak, SSDP) also emerges in silicate glasses. Figure 4 shows the position of the first two sharp diffraction peaks (SDPs) for amorphous  $\text{Mg}_2\text{SiO}_4$  in our study compared to previous static and shock data for  $\text{Mg}_2\text{SiO}_4$  and  $\text{MgSiO}_3$  as a function of pressure.

Our XRD data for shock-compressed  $\text{Mg}_2\text{SiO}_4$  shows values and trends similar to the dynamic- and static-compression data for  $\text{MgSiO}_3$  [7,9,11] and static-compression data for  $\text{Mg}_2\text{SiO}_4$  glass [10]. The pressure dependence of the SDP positions provides evidence of structural modifications under compression. For  $\text{Mg}_2\text{SiO}_4$ , first SDP has been ascribed primarily to Mg-Mg and Mg-Si interactions, whereas the second SDP is associated with O-O and Mg-O interactions appearing at high pressure [10,12]. The FSDP and SSDP for  $\text{Mg}_2\text{SiO}_4$  and  $\text{MgSiO}_3$  show a similar trend with increasing pressure. Our results provide evidence for shock-induced amorphization of forsterite above 79 GPa. This contrasts with previous interpretations of continuum gas-gun data that suggest decomposition to crystalline periclase ( $\text{MgO}$ ) and bridgmanite ( $\text{MgSiO}_3$ ). In dynamic-compression experiments, transformation to an equilibrium or metastable crystalline assemblage over laser ( $\sim\text{ns}$ ) and/or gas-gun ( $\sim\mu\text{s}$ ) timescales may be inhibited by low ionic diffusivity in the solid state. As a result of this kinetic limitation, a shocked sample may adopt a metastable amorphous structure as an intermediate state. It is worth noting that our results on forsterite above 80 GPa are also similar to those reported on single-crystal enstatite where amorphization is also observed at similar high stresses ( $>80\text{-}128$  GPa) but below the expected melting pressure [7], further evidence for the corresponding behavior of enstatite and forsterite under shock loading.

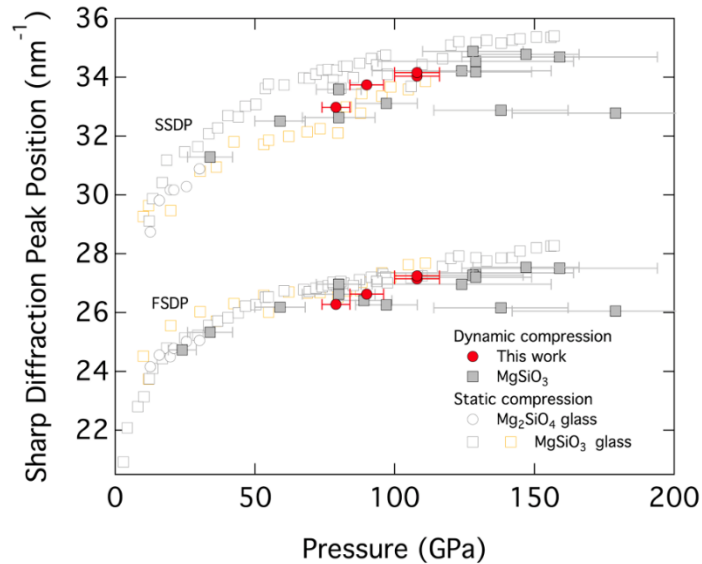


**Figure 4.** Position of the first (FSDP) and second (SSDP) amorphous diffraction peaks for shocked-compressed [010], [001] and polycrystalline forsterite (red circles) compared to laser-shock data for  $\text{MgSiO}_3$  (gray squares) [7,9] and static-compression data (open symbols) for  $\text{Mg}_2\text{SiO}_4$  [10] and  $\text{MgSiO}_3$  (gray: [9] glasses).

## Summary

The phases adopted by forsterite under laser-driven shock loading to 19 – 122 GPa were determined by X-ray diffraction. Our results indicate that forsterite and the metastable polymorph forsterite III coexist from ~33 to 75 GPa along the Hugoniot. This is generally consistent with a previous X-ray diffraction study using gas-gun experiments. The lattice parameters and densities of forsterite and forsterite III under compression determined from our shock data are consistent with values from continuum gas-gun data, as well as static-compression and gas-gun X-ray diffraction studies.

Higher stress behavior under dynamic loading depends on the initial crystal orientation. Polycrystalline forsterite undergoes amorphization above 79 GPa, but the [100]- and [001]-oriented single crystals show only partially disordered structures at 108 GPa. For the [100] orientation, an unknown crystalline phase occurs up to 122 GPa. For amorphous  $Mg_2SiO_4$  at 79–108 GPa, two sharp diffraction peaks are observed, which are consistent with values for amorphous  $Mg_2SiO_4$  and  $MgSiO_3$  under static compression and  $MgSiO_3$  under dynamic compression.

This study provides new insight into the transformation of forsterite under nanosecond-duration shock loading. This work emphasizes the importance of formation of metastable phases along the Hugoniot and adds to evidence that the 300-K single-crystal diamond anvil cell experiments have relevance for understanding structures formed under shock compression. In particular, the metastable phase forsterite III has now been shown to form under dynamic compression from 10s to 100s of nanoseconds as well as under 300-K static compression. Upon compression to higher pressures,  $Mg_2SiO_4$  transforms to an amorphous phase. These results have broad relevance for understanding the behavior of silicates under dynamic compression.

## Human Resources

This project provided training for two graduate students (D. Kim, and S. K. Han) and one postdoctoral fellow (E. J. Berryman). The project also supported an international collaboration with Dr. K. Appel (EuXFEL).

## Collaboration

This work was performed in collaboration with S. J. Tracy (Carnegie Institution for Science) R. F. Smith, M. C. Akin, and J. H. Eggert (Lawrence Livermore National Laboratory), C. A. Bolme (Los Alamos National Laboratory), A. Gleason, H. J. Lee, B. Nagler, and E. F. Cunningham (all at Stanford Linear Accelerator Center), S. Speziale (GFZ Potsdam), M. Schoelmerich and K. Appel (EuXFEL), V. B. Prakapenka (University of Chicago), J. K. Wicks (Johns Hopkins).

## Publications and Presentations

### Publications

Kim, D., S. J. Tracy, R. F. Smith, A. E. Gleason, C. A. Bolme, V. B. Prakapenka, K. Appel, S. Speziale, J. K. Wicks, E. J. Berryman, S. K. Han, M. Schölmerich, H. J. Lee, B. Nagler, M. Akin, P. D. Asimow, J. H. Eggert, and T. S. Duffy, Femtosecond X-ray diffraction of laser-shocked forsterite,  $\text{Mg}_2\text{SiO}_4$ , to 122 GPa, *Journal of Geophysical Research*, in press, 2020.

### Presentations

Kim, D., S. J. Tracy, R. F. Smith, A. E. Gleason, C. A. Bolme, V. B. Prakapenka, K. Appel, S. Speziale, J. K. Wicks, E. J. Berryman, S. K. Han, M. O. Schoelmerich, H. J. Lee, B. Nagler, E. F. Cunningham, M. C. Akin, P. D. Asimow, J. H. Eggert, and T. S. Duffy, Femtosecond X-ray Diffraction of Laser-shocked Forsterite ( $\text{Mg}_2\text{SiO}_4$ ) to 122 GPa, *American Geophysical Union Fall meeting*, , Dec. 2020.

Duffy, T.S., X-ray diffraction of phase transitions in shock-compressed minerals, *Advanced Photon Source High-Pressure Interest Group*, June 2020. (Invited)

Duffy, T.S., Structure, equation of state, and phase transitions in shock-compressed minerals to TPa pressures, 8<sup>th</sup> Joint Workshop on High Pressure, Planetary, and Plasma Physics, Dresden, Germany, Oct. 9-11, 2019 (Invited)

M. Schoelmerich, K. Appel, C. Bolme, T. Duffy, E. Galtier, A. Gleason, B. Nagler, T. Preston, R. Smith, S. Tracy, T. Tschentscher, L. Wollenweber, U. Zastraub, Structure of  $\text{SiO}_2$  Melts at Megabar Pressures, *European High-Pressure Research Group Meeting*, Prague, September 2019

D. Kim, S. J. Tracy, E. J. Berryman, S. K. Han, R. F. Smith, A. E. Gleason, C. A. Bolme, K. Appel, M. Schölmerich, V. B. Prakapenka, H. J. Lee, B. Nagler, P. D. Asimow, M. Akin, J.H. Eggert, and T. S Duffy, X-ray diffraction study of laser-shocked forsterite ( $\text{Mg}_2\text{SiO}_4$ ) from 20-130 GPa, *Topical Conference on Shock Compression of Condensed Matter*, Portland, June 2019.

Duffy T. S., In situ structural studies of shock-compressed minerals, *American Geophysical Union Fall Meeting*, Washington DC, December 2018.

D. Kim, S.J. Tracy, R.F. Smith, E. Berryman, S. Han, A.E. Gleason, C.A. Bolme, K. Appel, M. Schoelmerich, V.B. Prakapenka, H.J. Lee, B. Nagler, J.H. Eggert, and T.S. Duffy, High-pressure behavior of forsterite ( $\text{Mg}_2\text{SiO}_4$ ) under dynamic loading, *Sixth High-Powered Laser Workshop*, Stanford Linear Accelerator Center, September 2018.

## References

[1] A. E. Ringwood, *Phase Transformations and Their Bearing on the Constitution and Dynamics of the Mantle*, Geochim. Cosmochim. Acta **55**, 2083 (1991).

[2] G. J. Finkelstein, P. K. Dera, S. Jahn, A. R. Oganov, C. M. Holl, Y. Meng, and T. S. Duffy, *Phase Transitions and Equation of State of Forsterite to 90 GPa from Single-Crystal X-Ray Diffraction and Molecular Modeling*, Am. Mineral. **99**, 35 (2014).

[3] J. L. Mosenfelder, P. D. Asimow, and T. J. Ahrens, *Thermodynamic Properties of  $Mg_2SiO_4$  Liquid at Ultra-High Pressures from Shock Measurements to 200 GPa on Forsterite and Wadsleyite*, J. Geophys. Res. **112**, B06208 (2007).

[4] M. G. Newman, R. G. Kraus, M. C. Akin, J. V. Bernier, A. M. Dillman, M. A. Homel, S. Lee, J. Lind, J. L. Mosenfelder, D. C. Pagan, N. W. Sinclair, and P. D. Asimow, *In Situ Observations of Phase Changes in Shock Compressed Forsterite*, Geophys. Res. Lett. **45**, 8129 (2018).

[5] B. Nagler, B. Arnold, G. Bouchard, R. F. Boyce, R. M. Boyce, A. Callen, M. Campell, R. Curiel, E. Galtier, J. Garofoli, E. Granados, J. Hastings, G. Hays, P. Heimann, R. W. Lee, D. Milathianaki, L. Plummer, A. Schropp, A. Wallace, M. Welch, W. White, Z. Xing, J. Yin, J. Young, U. Zastrau, and H. J. Lee, *The Matter in Extreme Conditions Instrument at the Linac Coherent Light Source*, J. Synchrotron Radiat. **22**, 520 (2015).

[6] Y. Zhang, Y. Zhang, Y. Liu, and X. Liu, *A Metastable Fo-III Wedge in Cold Slabs Subducted to the Lower Part of the Mantle Transition Zone: A Hypothesis Based on First-Principles Simulations*, Minerals **9**, 186 (2019).

[7] J. -A. Hernandez, G. Morard, M. Guaraguaglini, R. Alonso-Mori, A. Benuzzi-Mounaix, R. Bolis, G. Fiquet, E. Galtier, A. E. Gleason, S. Glenzer, F. Guyot, B. Ko, H. J. Lee, W. L. Mao, B. Nagler, N. Ozaki, A. K. Schuster, S. H. Shim, T. Vinci, and A. Ravasio, *Direct Observation of Shock-induced Disordering of Enstatite below the Melting Temperature*, Geophys. Res. Lett. **47**, (2020).

[8] G. J. Finkelstein, P. K. Dera, and T. S. Duffy, *Phase Transitions in Orthopyroxene ( $En_{90}$ ) to 49 GPa from Single-Crystal X-Ray Diffraction*, Physics of the Earth and Planetary Interiors **244**, 78 (2015).

[9] G. Morard, J.-A. Hernandez, M. Guaraguaglini, R. Bolis, A. Benuzzi-Mounaix, T. Vinci, G. Fiquet, M. A. Baron, S. H. Shim, B. Ko, A. E. Gleason, W. L. Mao, R. Alonso-Mori, H. J. Lee, B. Nagler, E. Galtier, D. Sokaras, S. H. Glenzer, D. Andrault, G. Garbarino, M. Mezouar, A. K. Schuster, and A. Ravasio, *In Situ X-Ray Diffraction of Silicate Liquids and Glasses under Dynamic and Static Compression to Megabar Pressures*, Proc. Natl. Acad. Sci. U.S.A. (2020).

[10] C. J. Benmore, E. Soignard, M. Guthrie, S. A. Amin, J. K. R. Weber, K. McKiernan, M. C. Wilding, and J. L. Yarger, *High Pressure X-Ray Diffraction Measurements on  $Mg_2SiO_4$  Glass*, J. Non-Cryst. Solids **357**, 2632 (2011).

[11] Y. Kono, Y. Shibasaki, C. Kenney-Benson, Y. Wang, and G. Shen, *Pressure-Induced Structural Change in  $MgSiO_3$  Glass at Pressures near the Earth's Core–Mantle Boundary*, Proc. Natl. Acad. Sci. U.S.A. **115**, 1742 (2018).

[12] O. Adjaoud, G. Steinle-Neumann, and S. Jahn,  *$Mg_2SiO_4$  Liquid under High Pressure from Molecular Dynamics*, Chem. Geol. **256**, 185 (2008).